drones

MDPI

Article

UAV–UGV Formation for Delivery Missions: A Practical Case Study

Leonardo A. Fagundes-Júnior [1,†], Celso O. Barcelos [1,†], Amanda Piaia Silvatti [2] and Alexandre S. Brandão [1,*,‡]

[1] Núcleo de Especialização em Robótica, Programa de Pós-Graduação em Ciência da Computação, Departamento de Engenharia Elétrica, Universidade Federal de Viçosa, Viçosa 36570-900, MG, Brazil; leonardo.fagundes@ufv.br (L.A.F.-J.); celso.barcelos@ufv.br (C.O.B.)
[2] Laboratório de Análises Biomecânicas, Departamento de Educação Física, Universidade Federal de Viçosa, Viçosa 36570-900, MG, Brazil; amandasilvatti@ufv.br
* Correspondence: alexandre.brandao@ufv.br; Tel.: +55-31-3612-6540
† These authors contributed equally to this work.
‡ Current address: Av. Peter Henry Rolfs, Campus Universitário, Via da Agronomia, 299, Viçosa 36570-900, MG, Brazil.

Abstract: Robotic transport missions serve a variety of valuable purposes within similar contexts. These include delivering packages in urban or remote areas, dispatching supplies to disaster or conflict zones, and facilitating delivery operations. In such a context, this work deals with the cooperation and control of multiple-robot systems involving heterogeneous robot formation with sensing and actuation capabilities to perform load transportation tasks. Two off-the-shelf unmanned ground vehicles (UGVs) working cooperatively with one unmanned aerial vehicle (UAV) are used to validate the proposal. The interactions between the UAV and the UGVs are not only information exchanges but also physical couplings required to cooperate in the load's joint transportation. The existence of an obstacle between the two UGVs makes it impossible for them to meet each other. Thus, the lifting, transport, and delivery of the load from one UGV to the other are performed by a UAV with a suspended electromagnet actuator. Experiments are performed for a weight of 165 g (load + electronic board), which corresponds to up to 36% of the UAV's mass.

Keywords: multi-robot systems; route planning and following; pick-and-place; autonomous systems

Academic Editors: Weiran Yao, Xiangyu Shao, Yuehua Liu, Liming Xin and Jiatao Ding

Received: 14 December 2024
Revised: 4 January 2025
Accepted: 8 January 2025
Published: 11 January 2025

Citation: Fagundes-Júnior, L.A.; Barcelos, C.O.; Silvatti, A.P.; Brandão, A.S. UAV–UGV Formation for Delivery Missions: A Practical Case Study. *Drones* **2025**, *9*, 48. https://doi.org/10.3390/drones9010048

1. Introduction

The automation of delivery processes using unmanned aerial vehicles (UAVs) stands out due to the high levels of execution accuracy and velocity of such robots compared to the traditional model of delivery, using manned vehicles on the ground [1]. Delivery companies are seeking faster and more cost-effective methods for parcel distribution [2]. Allied to this, the rapid advancement of aerial robot technologies is promoting a migration in the use of UAVs from passive tasks, such as inspection and monitoring, to active ones, such as cargo manipulation and transportation [3–5]. Thus, such devices can be incorporated into the parcel delivery industry in a time- and cost-efficient manner.

It is important to highlight that robot modeling and control are influenced by the flight mode—whether lifting, transporting, or delivering—each of which exhibits unique dynamic characteristics affected by the weight and shape of the payload [6,7]. These issues have motivated several research groups to investigate the potential of multi-agent systems in order to overcome such limitations [8,9]. The use of multiple UAVs carrying a single payload is a way to avoid some complexities using sub-optimal and non-agile motions

or simplified models [10–14], distributing the cargo weight and reducing disturbances to the aerial vehicle during transport. However, for long-distance missions, the battery consumption may become the biggest villain. Therefore, these tasks can be more effectively accomplished by employing heterogeneous robotic agents with varying capabilities.

1.1. Related Works

Recent advances in the control of multi-robot systems have showcased the potential for synergistic collaboration between a UAV and static or mobile platforms, such as unmanned ground vehicles (UGVs). The integration of UAVs and UGVs into collaborative systems has opened up new opportunities for dealing with complex tasks that require both aerial and ground perspectives. UAVs excel at rapid deployment and providing comprehensive aerial views, while UGVs offer detailed ground-level interaction and manipulation capabilities [15,16]. In cargo transportation scenarios, UAVs facilitate quick and agile deliveries, while UGVs are better suited to handling heavier loads due to their greater load capacity. However, UGVs are often limited by road networks, while UAVs, despite their ability to traverse diverse terrain, face energy limitations [17]. They both ultimately need route scheduling to optimize delivery to the customer. By exploiting their unique strengths in unified structures, these systems provide innovative solutions for missions that require both aerial and ground resources, offering significant advantages in various applications due to the complementary nature of these robots [18,19].

Despite significant progress, UAV–UGV collaboration continues to face critical challenges in key areas, such as computational constraints due to the size and weight limitations of UAVs and UGVs, which reduce their computational power, making real-time operations difficult or even unfeasible. Additionally, communication network instability disrupts seamless interaction and effective collaboration among the agents, directly affecting coordination complexity, which increases with the number of agents. Furthermore, when physical barriers are present in the environment, complex scenarios involving challenging terrains or unforeseen environmental conditions require advanced planning and adaptability. In addressing these challenges, researchers aim to optimize the potential of collaborative UAV–UGV systems to ensure they operate reliably and efficiently in real-world applications.

In such a context, a notable and emerging application of UAV–UGV cooperation for load transportation is in last-mile delivery scenarios. These applications involve UAVs delivering packages [20–23], UAVs taking off and landing on trucks navigating street networks [24–27], and deliveries determined by consumer preferences or predefined delivery modes, completed by either trucks or drones [28]. With many countries approving regulations enabling the use of small drones for package delivery, the last-mile package delivery problem—requiring the autonomous navigation of UGVs and UAVs—has garnered significant global research attention. However, achieving such tasks demands a high degree of autonomy, alongside a control system capable of maintaining formation during navigation and dynamically rerouting to safe paths when obstacles obstruct the original route. Within this context, the current study simulates the final step of a package delivery scenario, focusing on the stage where the UAV must land back on a mobile terrestrial platform (e.g., a small truck) after delivering its payload. Specifically, this work examines the phase just prior to the UAV's landing, under the assumption that only the UGV encounters obstacles.

Given the limitations of a single robot, whether a UAV or a UGV, for load transportation, the collaboration between these mechanisms to enhance their real-world applications has increasingly attracted the attention of researchers in recent years. Arbanas et al. [29] present a heterogeneous formation composed of UAVs and UGVs in cooperation to accomplish load transportation missions. The UAV, equipped with two manipulator arms, is

designed to pick up or deliver a load onto a UGV while navigating through an environment with obstacles. In this setup, all robots have access to information about the load's initial and final positions, as well as a 3D occupancy map of the environment. This work presents a high-level task-planning framework that enhances the unique capabilities of ground and aerial robots to enhance their cooperative capabilities. Additionally, a task decomposition method is employed to coordinate the robots' movements, with their actions being guided by Generalized Partial Global Planning. Following this, the same research group presents in [30] a parcel transportation mission for a symbiotic multi-robot system composed by an aerial manipulator cooperating with a lightweight UGV (L-UGV). Such work proposes a decentralized control, tackling low-level and high-level structures. The first phase encompasses mapping and localization, motion planning for both the UAV and UGV, the UAV landing on the L-UGV, and the pick-up of the L-UGV. The second one focuses on decentralized ad hoc reasoning to determine the required actions for mission execution.

Guérin et al. [31] propose a decentralized multi-robot strategy for load transportation in industrial environments, where the UAV and a human operator collaboratively guide the UGV team to move in a coordinated way. The UAV flies over the area to offer global coverage and assist the UGVs during navigation, avoiding obstacles. The human operator selects the waypoints. A camera mounted on the UAV is used to provide real-time localization information to a UGV, the leader, to navigate in the scenario while the other UGVs, the followers, take the leader as a target and follow it while carrying the loads.

A recent obstacle avoidance algorithm embedded in a formation controller to guide a heterogeneous UAV–UGV team in a path-following task, making it possible to control the reference path velocity given to the robots, is presented in [27]. The UAV returns after delivering a package and needs to land on the UGV, its reference base, which will then proceed with its route toward another delivery goal. The formation is considered as a virtual structure. After executing the parcel delivery mission, the UAV lands on the UGV by modeling a straight line structure formed between the robots, in which the distance parameter decreases with time in order to bring them closer for a smooth and safe landing.

1.2. Aims and Contributions of the Work

Instead of building UAVs with better capabilities for load transportation, we propose a collaborative strategy involving a UAV and two UGVs. In such a multi-robot system, one UGV has a trailer for transporting the UAV and, consequently, for saving its battery life. Since the UGV is not able to easily overcome obstacles such as ditches and broken bridges, the use of the UAVs becomes a feasible solution. Specifically, the highlights of the proposal's contributions are as follows:

- High-level decentralized mission planning for a UGV–UAV formation cooperatively working in transportation missions under environment constraints.
- The development of a lightweight electromagnet actuator driven by an Arduino Nano microcontroller.
- Validation in real-world experiments, allowing for success in accomplishing the picking/delivery of cargo from/on moving UGVs.

To address these topics, this paper is organized as follows: Section 2 provides a detailed explanation of the proposed mission planning algorithm and its integration with the multi-robot system for load transportation. Section 3 outlines the experimental setup, including the electronic module of the actuation system and the path parameters for the robots. Subsequently, Section 4 presents the results of experiments conducted using the unicycle-like mobile platform (UGV) and the quadrotor (UAV), highlighting the robots' behavior during navigation and discussing practical issues related to perception and navigation. Finally, Section 5 summarizes the key findings and discusses future research directions.

2. Mission Planning for Last-Mile Delivery Application

The load transportation plan studied here is designed for environments where it is impossible for the ground robot to reach the other side of the map due to obstacles such as a river, ditch, steep mountain, landslide, or broken bridge, among others. As a result, the cargo must be transported from one side to the other, as illustrated in Figure 1. Therefore, UAV–UGV cooperation emerges as a valuable approach.

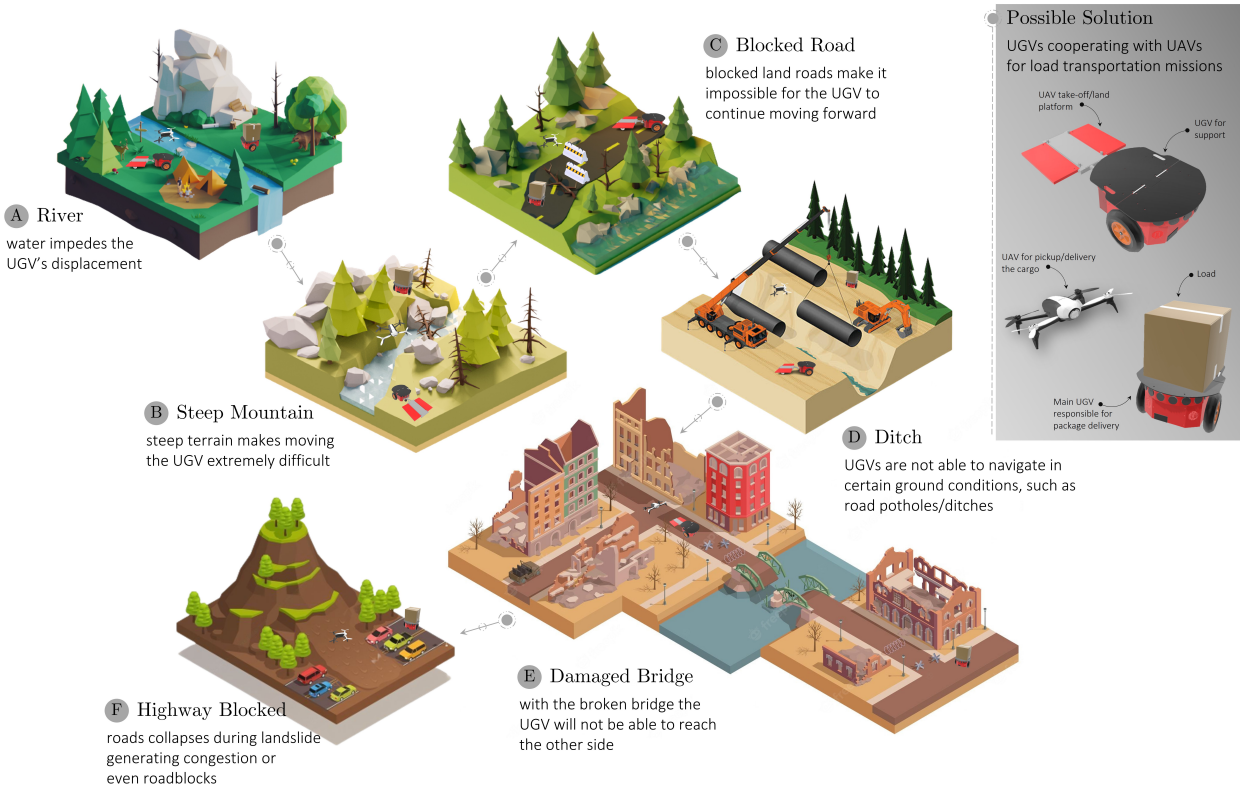

Figure 1. UGV load transportation limitations due to specific environment constraints. A possible solution for delivery packets in long-distance missions is the cooperation between UAV and UGVs in the mission planning step.

In summary, the UGV carrying the cargo identifies the obstacle ahead and communicates with the ground control station (GCS), requesting support to complete the mission in a timely manner. Upon receiving the support request, GCS sends a command to one of its bases containing robots on standby. The UAV–UGV robot team with the highest availability departs to the estimated location of the other UGV to collect the payload and continue the mission.

The main idea is that the UGVs are required to perform deliveries and must travel long distances with the loads. However, they may encounter obstacles along the way that make it impossible to go ahead with the delivery or that delay the transport. Thus, when identifying the impossibility of completing the mission, the robot responsible for the delivery sends a support request to the GCS closest to the final delivery destination city. The operator responsible for managing the system will open an order to send the robots with the highest availability among those available at the location. As the impediment to the mission of the main UGV is due to the presence of an obstacle in the way, the use of a UAV is essential for the collection of the cargo from the UGV that requested support, and delivery to the supporting UGV is of paramount importance. Thus, the UGV that departs on the rendezvous with the main UGV carries with it a UAV capable of tracking the main UGV and collecting the cargo it carries.

This work proposes a collaborative approach between aerial and terrestrial robots for scenarios involving package transport and delivery, aiming to optimize the unique characteristics of each type of robot and minimize the mission execution time. The evaluation focused on a proof-of-concept experiment for last-mile delivery in a controlled environment, featuring an aerial robot, two ground robots, and a load. While the study successfully demonstrates this collaboration in a simplified model, when it comes to real-world applications, the scenarios often involve larger and more robust vehicles, such as trucks and drones with a greater payload capacity and autonomy. In such cases, the presence of unexpected obstacles must be addressed, requiring strategies for obstacle identification and analysis of the ground robot's ability to either overcome or avoid them to minimize energy consumption and task completion time. This remains a suggestion for future work to enhance the robustness and practicality of the proposed architecture.

2.1. Robot Modeling and Control

2.1.1. The Pioneer P3-Dx UGV

In this work, we utilized the Pioneer P3-Dx, a unicycle-like mobile robot, whose kinematic model is described as shown in Figure 2. Given that navigation occurs solely in the horizontal plane, the robot's pose is represented by the vector $\mathbf{x} = [x\ y\ \psi]^\intercal$, where x and y denote the coordinates of the control point located at the center of the virtual axle $\langle r \rangle$, and ψ represents its heading relative to the x axis in the inertial frame $\langle w \rangle$. The linear and angular velocities of the robot are denoted by u and ω, respectively, and the vector $\mathbf{u} = [u\ \omega]^\top$ comprises these velocities. The non-zero constant a denotes the distance from the origin of the body axes (the baseline connecting the two driven wheels) to the control point of interest. Additionally, the mobile robot seeks a goal with a specific orientation, represented by the reference frame $\langle g \rangle$.

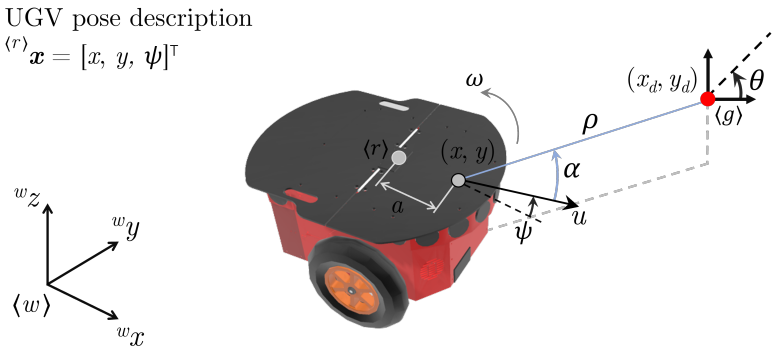

Figure 2. Spatial unicycle-type robot representation and polar modeling variables (in blue). The target point is represented by $\mathbf{x}_d = [x_d\ y_d\ \psi_d]^\intercal$.

The system of kinematics equations describing the motion of the robot over time in the Cartesian plane is presented in [32]. In most applications, especially those performed at high speeds, the robot's kinematic model alone is not able to track and follow trajectories and/or paths efficiently and accurately. Thus, for the design of motion controllers, it is of paramount importance to consider the robot's dynamic modeling. This UGV has an embedded low-level controller that drives the two motors of the vehicles, enabling the use of the aforementioned high-level commands of linear and angular velocities, $\mathbf{u}$. To deal with the dynamic effects caused by inertia and friction, a dynamic model first introduced in [33] and updated in [34] was used.

The robot dynamic model in the compact form is presented by [35] as

$$\mathbf{M}\dot{\mathbf{u}} + \mathbf{C}\mathbf{u} = \mathbf{u}_{ref}, \tag{1}$$

where **M** and **C** are the Inertia and Coriolis matrices, respectively.

A positioning control can be achieved using inverse kinematics and considering a desired trajectory. The reference velocity command can be defined as

$$\mathbf{u}_d = \mathbf{K}^{-1}(\tanh(\dot{\tilde{\mathbf{x}}}) + \mathbf{K}_p \tanh(\tilde{\mathbf{x}})), \tag{2}$$

where $\mathbf{K}_p$ is a positive definite gain matrix.

To contemplate applications in which the robot needs to navigate under high-speed movements, and to evaluate a more realistic scenario, a dynamic compensation module is adopted. Considering the (1), the adopted dynamic compensation control law is given by

$$\mathbf{u}_{ref} = \mathbf{M}(\dot{\mathbf{u}}_d + \kappa(\mathbf{u}_d - \mathbf{u}) + \mathbf{C}\mathbf{u}) \tag{3}$$

in which the gain κ is a positive definite matrix and $(\mathbf{u}_d - \mathbf{u})$ is the velocity tracking error. The control signal $\dot{\mathbf{u}}_u$ is obtained by numeric differentiation considering the sampling time of the control loop.

Now, the use of the proposed dynamic model and its properties is illustrated via the design of an dynamic compensation controller. It receives the desired control signals $\mathbf{u}_d$ from the kinematic controller and generates a pair of linear and angular velocity references $\mathbf{u}_{ref}$ for the robot servos, as shown in the diagram block of Figure 3.

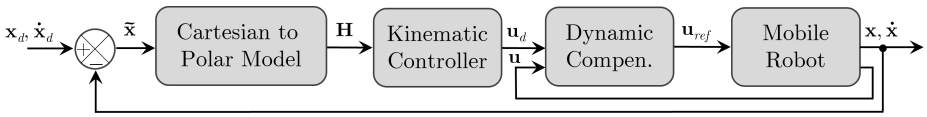

Figure 3. The dynamic control system in charge of guiding the robot to the target point.

2.1.2. The Parrot Bebop 2 UAV

To model the the UAV used in this work, we will refer to the description presented in Figure 4. The translational coordinates of the quadrotor are represented as $\mathbf{x} = \begin{bmatrix} x & y & z \end{bmatrix}^\top$ and its attitude is described by the vector $\boldsymbol{\eta} = \begin{bmatrix} \phi & \theta & \psi \end{bmatrix}^\top$, which contains the roll, pitch, and yaw Tait–Bryan angles, both related to inertial reference frame $\langle w \rangle$. The Newton–Euler dynamics correspondent to the used quadrotor, and its simplified form is presented in Reference [35]. Such a simplification performs well for roll and pitch angles up to approximately 30°, corresponding to linear velocities of approximately 1.5–2 m/s [36]. In this way, the drone's dynamic model can be succinctly and simplified, expressed as

$$\begin{bmatrix} \ddot{x} \\ \ddot{y} \\ \ddot{z} \\ \ddot{\psi} \end{bmatrix} = \begin{bmatrix} k_1 c_\psi & -k_3 s_\psi & 0 & 0 \\ k_1 s_\psi & k_3 c_\psi & 0 & 0 \\ 0 & 0 & k_5 & 0 \\ 0 & 0 & 0 & k_7 \end{bmatrix} \begin{bmatrix} u_{v_x} \\ u_{v_y} \\ u_{\dot{z}} \\ u_{\dot{\psi}} \end{bmatrix} - \begin{bmatrix} k_2 c_\psi & -k_4 s_\psi & 0 & 0 \\ k_2 s_\psi & k_4 c_\psi & 0 & 0 \\ 0 & 0 & k_6 & 0 \\ 0 & 0 & 0 & k_8 \end{bmatrix} \begin{bmatrix} v_x \\ v_y \\ \dot{z} \\ \dot{\psi} \end{bmatrix}. \tag{4}$$

Let us denote $c_\cdot = \cos(.)$ and $s_\cdot = \sin(.)$ for compact notation. We have $\ddot{\mathbf{q}} = \mathbf{F}_1\mathbf{u} - \mathbf{F}_2\mathbf{v}$. Here, $\mathbf{u} \in [-1, 1]$ represents the normalized control signals. Specifically, u_{v_x} and u_{v_y} correspond to pitch and roll commands, indirectly influencing the linear velocity along the x_B and y_B axes. Additionally, $u_{\dot{z}}$ and $u_{\dot{\psi}}$ are related to the inputs for $\dot{z}$ and $\dot{\psi}$, respectively. Finally, v_x, v_y, and $\dot{z}$ denote the linear velocities along the x, y, and z axes in the UAV body frame, while $\dot{\psi}$ represents the angular velocity around the z axis in the global frame.

It is important to emphasize that, although the model does not encompass the dynamics of the UAV, this formulation aims to illustrate the impact of high-level control signals on the vehicle's maneuvers.

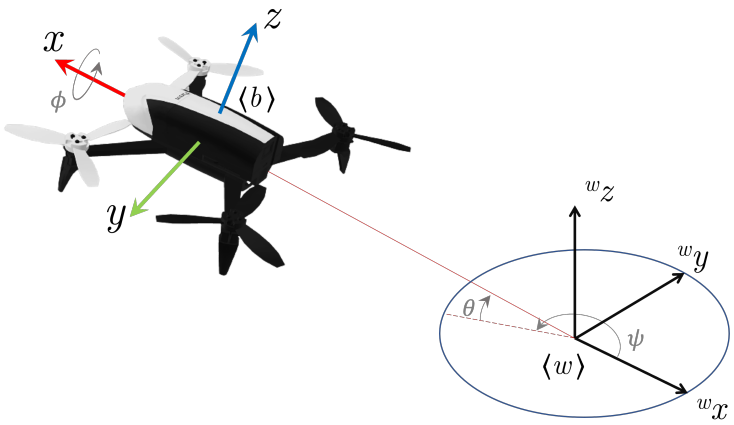

Figure 4. Parrot Bebop 2 description and pose variables, according to Tait–Bryan angle notation.

A near-hover model for the quadrotor can be written in the linear form:

$$\mathbf{u} = (\mathbf{F}\mathbf{K}_u)^{-1}(\ddot{\mathbf{x}}_{ref} + \mathbf{K}_{\dot{x}}\dot{\mathbf{x}}), \tag{5}$$

where $\mathbf{F}$ is a rotation matrix relating the coordinate systems $\langle w \rangle$ and $\langle b \rangle$, only dependent of ψ, and $\mathbf{x} = \begin{bmatrix} x & y & z & \psi \end{bmatrix}^\top$ are the displacements in frame $\langle b \rangle$ and yaw heading. The matrices $\mathbf{K}_u$ and $\mathbf{K}_{\dot{x}}$ are diagonal matrices containing, respectively, the dynamic and drag parameters for the model. The vector $\mathbf{x}_{ref}$ contains the reference control signal for a desired trajectory, and $\mathbf{u} = \begin{bmatrix} u_\theta & u_\phi & u_{\dot{z}} & u_{\dot{\psi}} \end{bmatrix}^\top$ is the vector of high-level commands, whose entries are all in the interval $[-1.0, +1.0]$.

The model parameters in $\mathbf{K}_u$ and $\mathbf{K}_{\dot{x}}$ are obtained through an identification procedure, as explained in [37]. Knowing such parameters, one can implement a feedback linearization controller, such that the reference signal $\dot{\mathbf{x}}_{ref}$ can be obtained using PD feedback plus a feedforward term, which corresponds to $\ddot{\mathbf{x}}_{ref} = \ddot{\mathbf{x}}_d + \mathbf{K}_d \tanh \dot{\tilde{\mathbf{x}}} + \mathbf{K}_p \tanh \tilde{\mathbf{x}}$. In this formulation, $\mathbf{x}_d$ is a trajectory to be tracked, $\tilde{\mathbf{x}} = \mathbf{x}_d - \mathbf{x}, \dot{\tilde{\mathbf{x}}} = \dot{\mathbf{x}}_d - \dot{\mathbf{x}}$, and $\mathbf{K}_d$ and $\mathbf{K}_p$ are positive definite gain matrices.

So, we can rewrite the control law in (5) as

$$\mathbf{u}_d = (\mathbf{F}\mathbf{K}_u)^{-1}(\ddot{\mathbf{x}}_d + \mathbf{K}_d \tanh \dot{\tilde{\mathbf{x}}} + \mathbf{K}_p \tanh \tilde{\mathbf{x}} + \mathbf{K}_{\dot{x}}\dot{\mathbf{x}}). \tag{6}$$

The diagram block describing the implemented controller is shown in Figure 5.

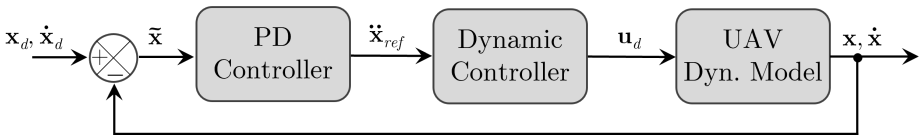

Figure 5. The dynamic control system in charge of guiding the robot to the target point.

For the successful experimental evaluation of the proposed high-level task allocation planner, all utilized robots must have the following prerequisite skills: dynamic stability for the preselected set of tasks and the ability to localize themselves, plan and execute obstacle-free trajectories, as well as an infrastructure through which they can share information and negotiate task allocation. The controllers presented for the UGV (3) and the UAV (6), were designed using the feedback linearization technique, which assumes perfect knowledge of the model parameters. Under these assumptions, the proposed controllers make the system asymptotically stable when closing the loop, as presented in [35].

In this work, we assume that the map of the environment is a priori known and that each vehicle knows its exact position. In practice, this is difficult to achieve without the utilization of self localization and map building algorithms. We leave this part of the system for future work and development, but, for now, we can achieve this through a combination of a motion tracking system and a priori known environment.

2.2. The Proposed Case Study for the Last-Mile Multi-Robot System

As aforementioned, UGVs have greater autonomy in the navigation time, a higher payload capacity, and greater traction. However, they often become stuck due to obstacles that cannot be circumvented, as well as suffer from sensory limitations and occlusions. On the other hand, UAVs provide a broad field of view and rapid coverage of search areas, making them ideal for mapping and monitoring tasks. Nevertheless, they are limited by their low payload capacity relative to their size, as well as a short operational flight time. However, the complementary skills offered by each vehicle can overcome the specific limitations of the other. Consequently, coordinated operations between UGVs and UAVs can generate highly advantageous synergies, including multi-domain sensing and improved line-of-sight communications. Thus, the objective here is to introduce a collaborative and exploratory approach using UGVs and UAVs.

Let us imagine a delivery agency that has regional branches (or headquarters) in cities strategically distributed to optimize the vehicle routing according to the goods to be transported. Each of these agency management and transportation posts has a number of unmanned vehicles available, capable of navigating autonomously to deliver the loads. All robots communicate with each of the GCSs, as suggested in Figure 6. In addition, all GCSs communicate with each other naturally and periodically in order to track the progress of deliveries. Operators are responsible for managing orders, deliveries, and keeping the entire system running. In our study and proof of concept, the miniature robots are Pioneer P3-DX and Bebop 2.Therefore, in order to prevent possible ambiguities, all images are referred to these robots, which here represent specialized vehicles for last-mile delivery missions.

To have an ideal and efficient system for outdoor load transportation, first, the proposed system focuses on autonomous UGV-UAV cooperation in an indoor monitored environment. Here, we focus on the autonomous last-mile delivery application in the presence of insurmountable obstacles by using only UGV robots.

2.3. The Cooperative Load Transportation Strategy

Figure 7 depicts an overview of the scenario configuration and the robots used in this work. For the moment, note that the markers used by the motion capture system are fixed in the robots to determine their posture in real time. To perform the missions, reference control signals for navigation are sent individually to the robots into the formation, closing the control loop. The vehicles' modeling and control are described in the following subsections. In order to facilitate understanding, the main UGV, responsible for cargo delivery, is referred to as **UGV A**, and the support UGV, which finishes the mission given by **UGV A** is labeled as **UGV B**. Finally, the aerial robot is referred to simply as **UAV**.

The last-mile delivery mission is planned considering that **UGV A** navigates in an obstacle-free environment, despite navigating in a reactive mode in order to adapt to the scenario conditions. To explain the stages of the task execution, we use the scenario presented in the center of Figure 7, which contains the UGVs and the UAV with their respective directions of movement, in addition to the load, the trailer platform, and the representative obstacle.

In the proposed approach, the decision for the UGV to remain in motion, rather than stopping and waiting for the UAV–UGV team to take over the load, is based on

optimizing the overall efficiency of the operation. By maintaining motion, the system minimizes idle time and ensures that the UAV can dynamically track and synchronize with the UGV, enabling a seamless and efficient load transfer process. This is particularly advantageous in scenarios where the UGVs are traveling in opposite directions or where mission completion time is critical. Stopping the UGV would introduce unnecessary delays and reduce the system's throughput, especially in situations involving multiple deliveries or tight operational deadlines. This continuous motion strategy exemplifies the benefits of collaboration between heterogeneous robots, taking advantage of the UAV's ability to adjust its trajectory and execute precise maneuvers to complete the load transfer efficiently.

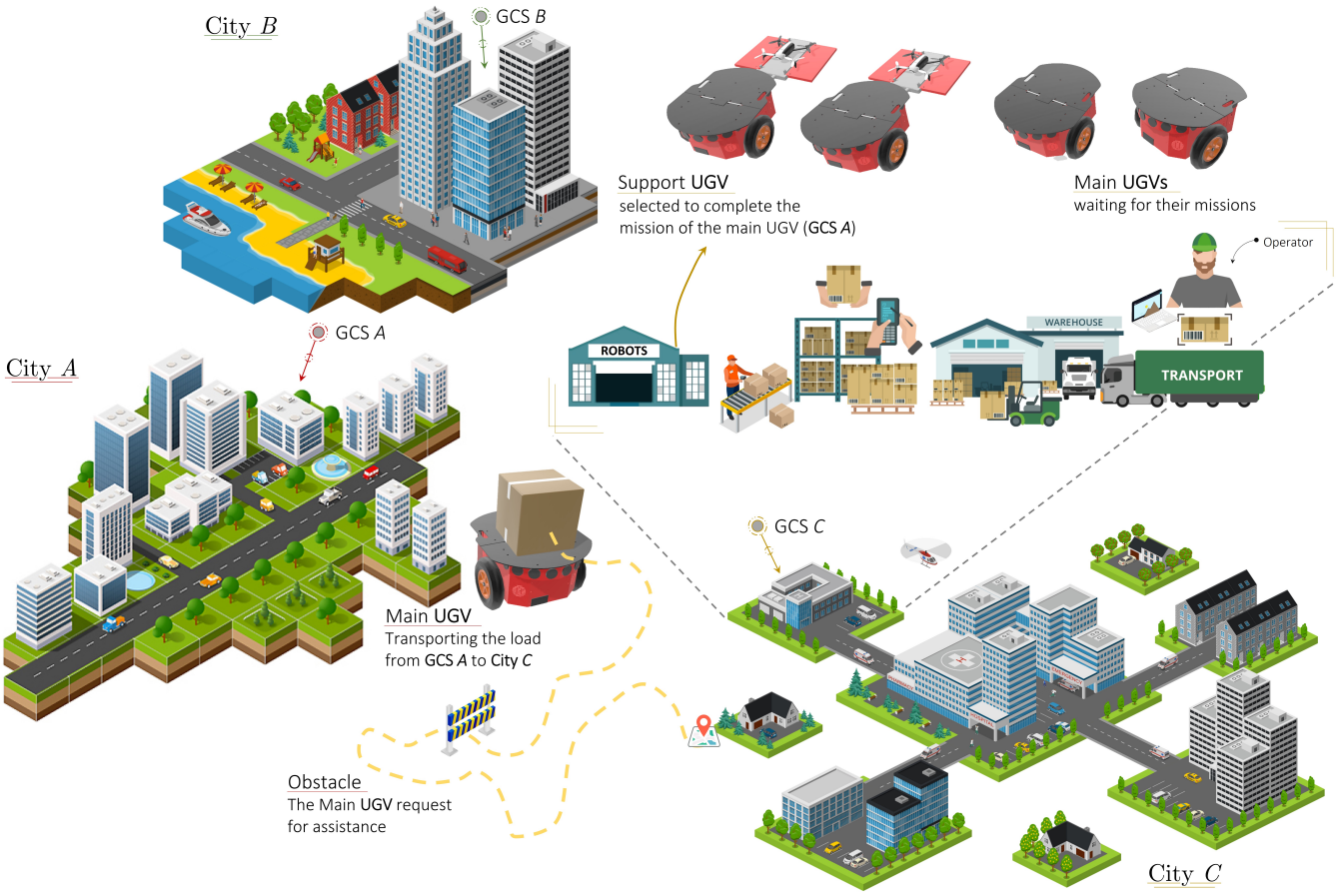

Figure 6. An example of a delivery agency and the route management proposed.

Our proposed strategy is split into six stages, illustrated in Figure 8 and explained below:

(i) **Setup**, Figure 8a: In the first step, **UGV A** receives its mission and initializes its movement with the load onboard. **UGV B** still waits for its task allocation;

(ii) **Assistance**, Figure 8b: **UGV A** faces an obstacle ahead and emits a request for assistance. While it reduces its velocity, a meeting request is sent to **UGV B**;

(iii) **Collect Cargo**, Figure 8c: **UAV** collects the load on **UGV A**, while both the UGVs remain in motion. **UAV** takes off from **UGV B** and moves toward **UGV A** to identify and pick up the transported load;

(iv) **Delivery**, Figure 8d: **UAV** collects the load and transports it to the moving **UGV B**, estimating its instantaneous position and velocity to delivery the load on it with precise accuracy;

(v) **Successful Mission**, Figure 8e: Once its pickup-and-delivery mission is successfully completed, **UAV** delivers the load on top of **UGV B** and prepares to land on the trailer. Meanwhile, **UGV A** continues its movement;

(vi) **Go Home**, Figure 8f: **UGV A** and **B** return to their GCS or perform a last-mile delivery mission.

To clarify, in our proposed system, the mission of the robot formation (UAV–UGV B) that collects the loads is defined by the GCS. Depending on the operational requirements, the UGV may perform either of the following:

- Cooperate with the UAV to perform a last-mile delivery directly to the customer.
- Navigate back to the GCS or a designated hub to transfer the packages for further processing or delivery.

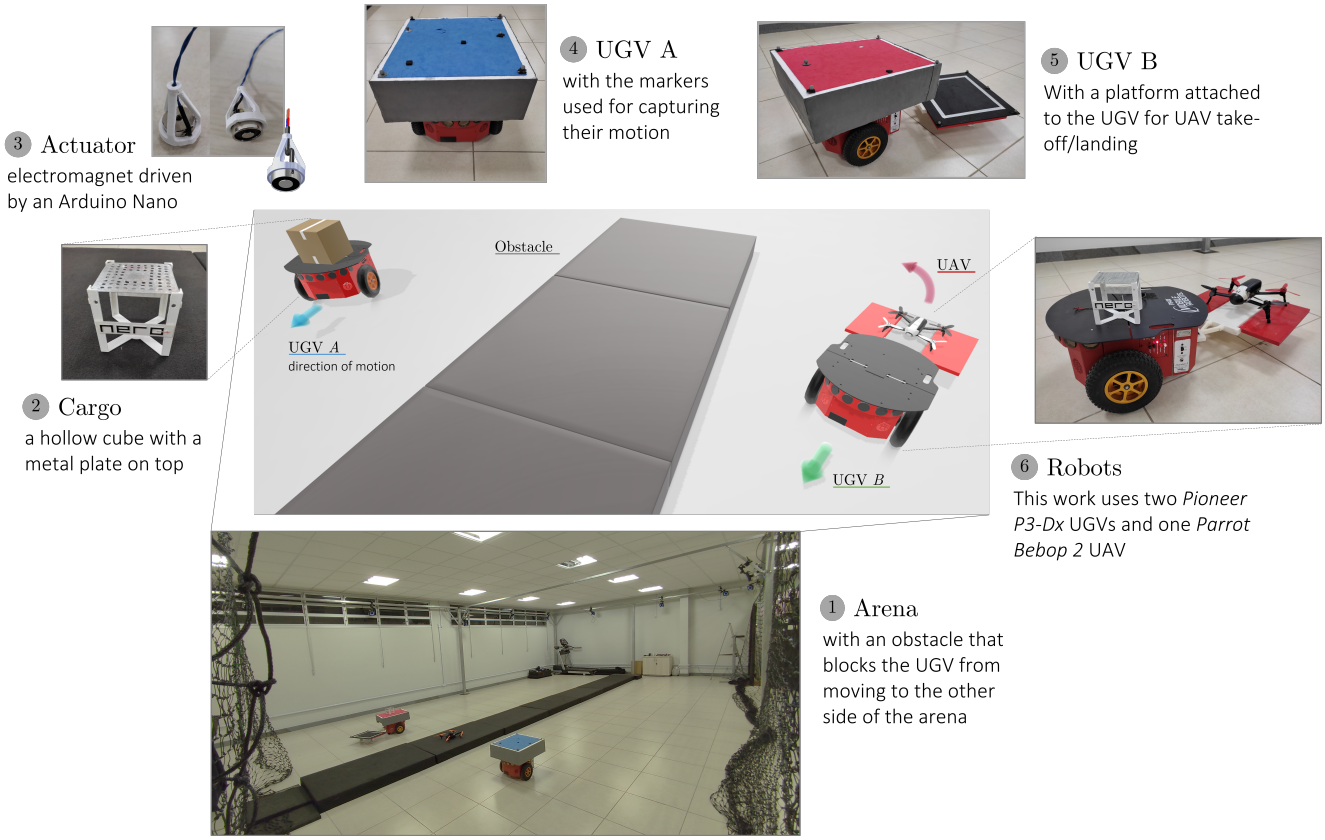

Figure 7. Mission scenario description and the robots used in this work. Image (**1**) shows the real-world scenario where the experiments were conducted. Images (**2**) and (**3**) highlight the load and the actuator, respectively. The real-world devices are depicted in images (**4**–**6**): the Pioneer 3-DX and its trailer, as well as the Bebop 2 UAV with the markers used for motion capture. Image (**6**) provides a complete view of all robots used in this work, including the UGV, UAV, cargo, and the trailer coupled to the UGV. At the center, the virtual representation used in subsequent discussions is illustrated.

The proposed approach focuses on scenarios where UGVs encounter obstacles that are impassable or inefficient to bypass. In environments with frequent or large obstacles, the deployment strategy could be optimized by pre-assessing the terrain using mapping and planning algorithms. For example, the UAV could be used proactively to survey the environment and identify the most efficient path for the UGVs while reserving its energy for critical load transfer tasks. This adaptive strategy will be explored in future work to enhance efficiency in complex environments.

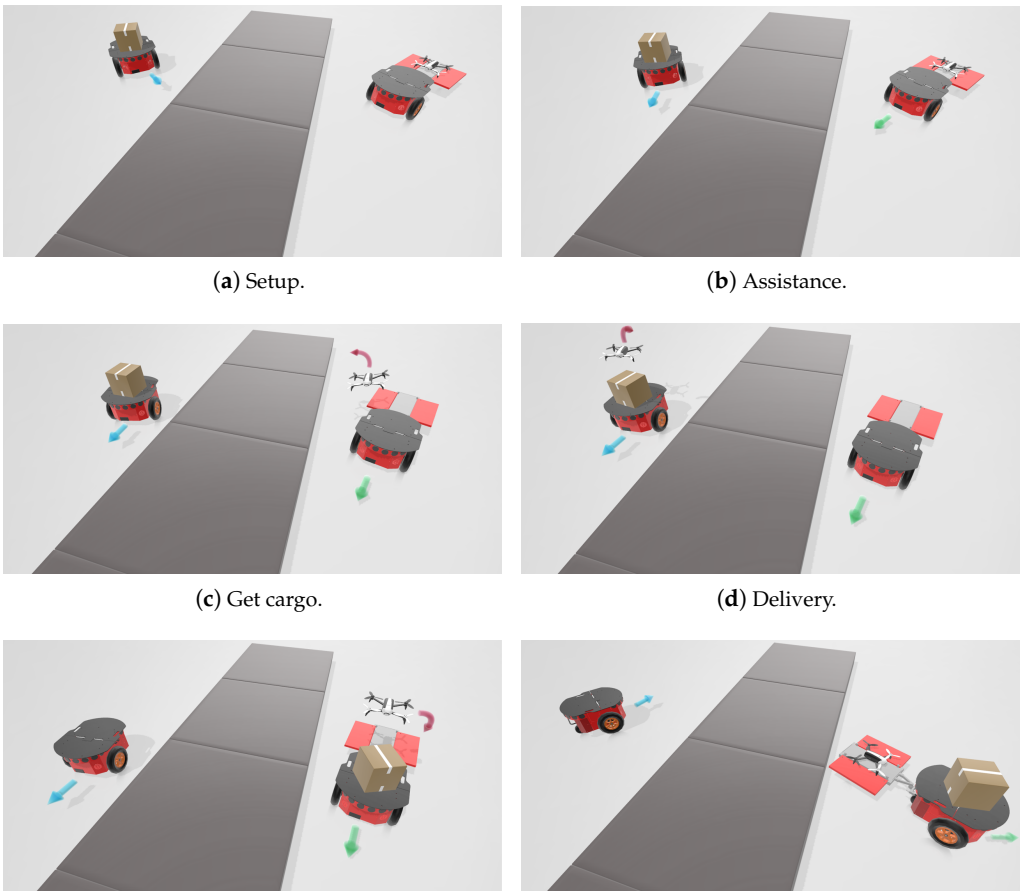

(**a**) Setup. (**b**) Assistance.

(**c**) Get cargo. (**d**) Delivery.

(**e**) Successful mission. (**f**) Go home.

Figure 8. The stages of the proposed UAV–UGV cooperation strategy for load transportation in hard-to-navigate terrestrial environments.

3. Experimental Setup

This section presents and analyzes a real experiment in which the UAV–UGV cooperation should perform a load transportation mission in the face of an obstacle. First, we briefly discuss the basic techniques and technologies used for our experimental setup, illustrated in Figure 9. As one can see, the UGVs are the nonholonomic unicycle Pioneer 3-DX mobile platform, and the UAV is the Parrot Bebop 2 quadrotor. To measure the vehicle positions along their navigation, the motion capture system *OptiTrack* is used. The high-level control code runs in MATLAB©. The algorithms run in an off-board station, at a rate of 30 Hz, computing the control signals that are sent to the robots via the ROS (Robot Operating System). The communication between the ROS and MATLAB is achieved through the AuRoRA Platform (https://github.com/neroUFV, accessed on 7 January 2025), a proprietary MATLAB library, which emulates the necessary ROS nodes and topics. All robots run an Ubuntu distribution plus ROS to execute the high-level mission planner. The cargo, electromagnet, and trailer are represented by physical objects, which also have their positions captured by the *OptiTrack* system.

The load is a hollow cube, which can be filled with rectangular-shaped loads. Its top face has a metal plate, to enable magnetic interaction with the actuator. Once energized, the electromagnet creates a magnetic field capable of supporting up to 2.5 kg, which is about eight times the UAV payload capacity.

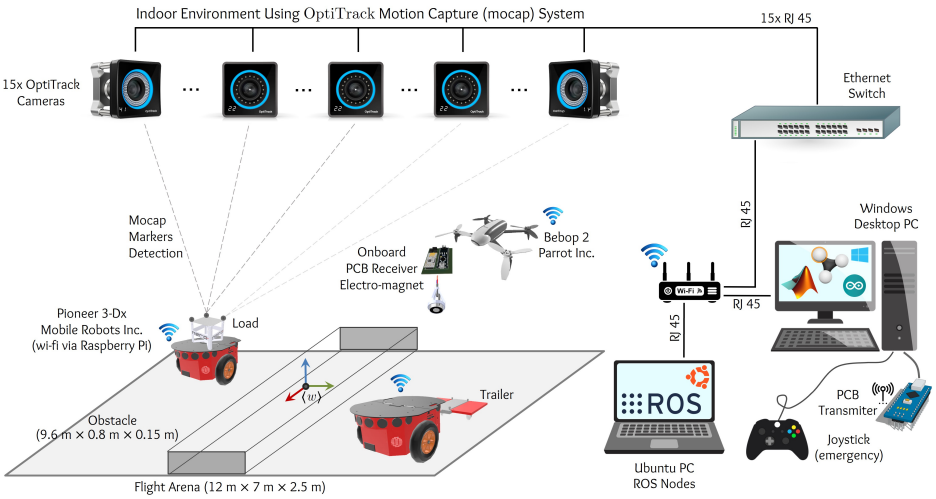

Figure 9. An overview of the hardware setup used to run the experiment. The Optitrack cameras compose the motion capture system, responsible for tracking all the rigid bodies in the arena.

3.1. Electronic Module of the Actuation System

The actuator introduced in Figure 7 is controlled by two modules using the *Arduino Nano* microcontroller. Our proposal consists of two printed circuit boards (PCB), named "Transmitter" and "Receiver". Both boards communicate through a Wi-Fi module attached to each PCB. At this point, it is important to mention that due to the distance and interference from very close communication channels, an antenna is attached to the Transmitter to increase the signal gain. This is necessary because the Receiver is onboard the UAV, which also communicates by Wi-Fi wireless network with the Ubuntu-ROS Master computer.

In order to drive the electromagnet and read the Receiver channels of the Wi-Fi module, the Transmitter PCB communicates directly with MATLAB via USB serial communication, as shown in Figure 10a. The main code sends a bit to the Transmitter indicating the moment to activate/deactivate the electromagnet. When reading the data received, the Transmitter sends a signal to the Receiver board. In turn, the Receiver PCB, besides the circuit to handle the data received from the Transmitter, also has a power module to supply the electromagnet when it receives the command to be activated, as can be seen in Figure 10b. In addition, Table 1 presents the list of components used for the development of the actuator system, both for the Transmitter PCB and the Receiver PCB.

It is worth noting that tasks such as lifting and transporting the load increase the UAV's energy consumption. However, this work demonstrates the feasibility of harnessing UAVs for short-duration tasks that are essential to mission success. Future optimizations could include the integration of energy-efficient path-planning algorithms and load-sharing strategies between the UAV and UGVs. For extended operations, hybrid UAV systems or charging stations positioned along the mission route could be implemented to address energy limitations.

For the purpose of optimizing the battery use of the actuator system, a strategy for operating the electromagnet is proposed here, which is represented in Figure 11. Once the current posture of the load and the electromagnet is known, it is possible to determine the distance between both objects. If this distance is lesser than a threshold, the solenoid actuates and attaches the load. Notice that this strategy prevents the electromagnet from being activated if the UAV misses the target and also ensures battery savings. In addition, such an approach can be understood as a volume over the metal plate where the electromagnet can be activated, as can be seen in Figure 11b.

Table 1. List of components for Transmitter (T) and Receiver (R).

Quantity	Item	PCB
2	Arduino Nano R3.0	T/R
2	Wireless Module Nrf24l01 2.4 GHz	T/R
1	Transistor BC 548 B	R
2	LED	T
1	Push Button	T
4	Resistors	T/R
1	Electromagnet/Solenoid 20 mm	R
-	PCB Pin Header Male/Female Connector	T/R

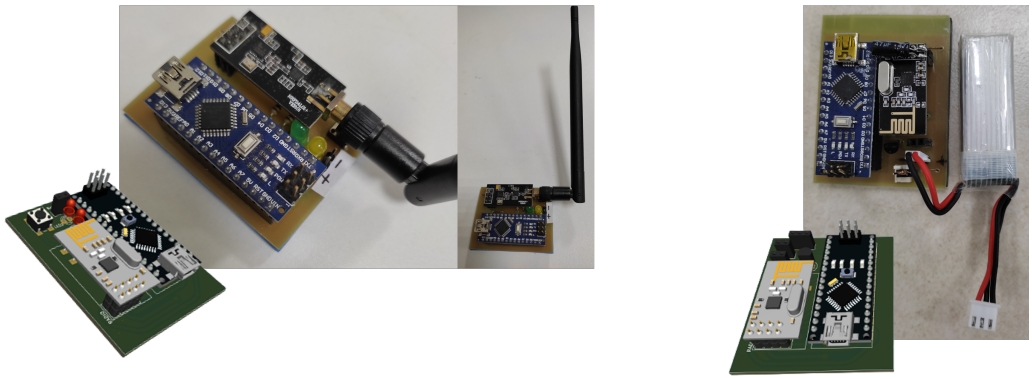

(**a**) (**b**)

Figure 10. Electromagnet PCBs: (**a**) Transmitter. (**b**) Receiver.

Similarly, to deliver the load onto the UGV, the position of the load is monitored relative to the geometric center of the ground robot. Thus, the load is only delivered if it can be guaranteed that it is within a safe region.

The precision positioning capability of the drone and ground robots is crucial for the successful execution of object capture and precision landing tasks in the proposed system. In this context, several methodologies can be employed to enhance the accuracy of positioning and control during operation. For instance, visual markers such as ArUco or AprilTags are widely used for robust and reliable object detection and pose estimation, both for load transportation [38–41] and autonomous landing [42–44]. These markers provide clear patterns that can be easily recognized by the drone's onboard camera, enabling the accurate localization of the load and landing platform. Additionally, feature-based methods, such as those leveraging Scale-Invariant Feature Transform (SIFT) or Speeded-Up Robust Features (SURF), can identify distinct features of the objects and environment, further improving the positioning accuracy. Recently, deep learning models have been increasingly adopted for visual-based pose estimation, offering improved performance in dynamic and complex environments [7].

Despite their effectiveness, these methods face certain limitations in real-world scenarios. For example, visual markers require proper placement and may be affected by lighting conditions, reflections, or occlusions. Similarly, feature-based approaches can struggle in low-texture or uniform environments, where distinct features are scarce. Deep learning models, while powerful, demand significant computational resources and may require extensive training data tailored to the specific operating environment. To mitigate these challenges, sensor fusion techniques, combining data from cameras, inertial measurement units (IMUs), and LiDAR, can be employed to enhance the localization accuracy and robustness.

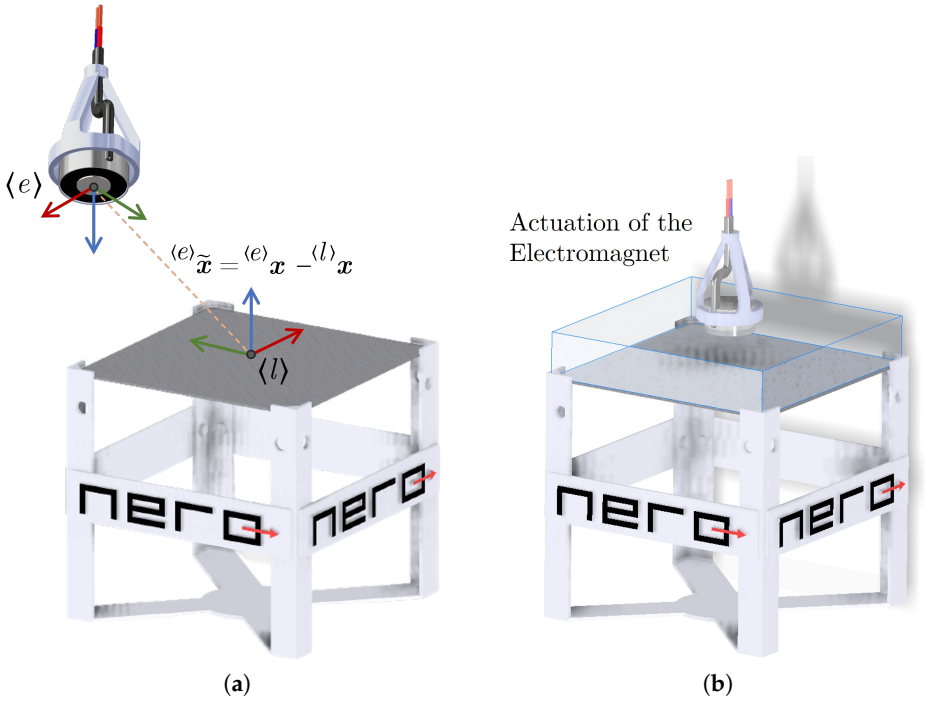

Figure 11. The actuator control strategy: (**a**) Error measurement. (**b**) Situation in which the electromagnet will be activated to pick up the cargo.

Moreover, real-world applications often involve external factors such as wind disturbances, vibrations, and varying terrains that further complicate precision positioning. These factors necessitate the development of adaptive control strategies to ensure stable operation under diverse conditions. By integrating advanced sensing and control methodologies, the system's reliability can be significantly improved, paving the way for practical deployments in urban and industrial environments. This discussion underscores the importance of evaluating and addressing real-world limitations to enhance the applicability and contribution of the proposed system.

The physical couplings used in this work are designed to simplify the attachment and detachment processes during load transfers, relying on an electromagnet actuator. We acknowledge that this introduces mechanical complexity and potential failure points. To mitigate this, future iterations of the system can explore alternative coupling mechanisms, such as soft robotic grippers or magnetic couplings with redundant systems, to enhance reliability. Additionally, predictive maintenance strategies could be integrated to monitor and prevent failures in critical components.

3.2. Path Parameters for the Robots

A robot can accomplish a load transportation task after traveling by a set of waypoints or after following a predefined path. In this work, we choose line- and super-ellipse-shape (also known as a Lamé curve) paths. Each one is better described in Table 2. For all of them, we consider $v_p = 0.7$ m/s if the path is followed by a UAV, and $v_p = 0.4$ m/s if the path if followed by a UGV. For the line-shape path, the α_p is a parametrization factor used to construct a trajectory with initial and final velocities equal to zero, where t is the current time, and t_f the trajectory final time. x_i and x_f are the initial and final UGV desired positions.

The Land Path is a line-shape trajectory to position the UAV immediately behind the trailer platform (which is moving), and perform a smooth and precise landing on it, anticipating its movement velocity. It is important to mention that the trailer movement must be estimated for a safe and smooth landing.

Table 2. Load transportation paths.

Path-Shape	**Description**
Line	$\mathbf{x} = v_p\left([x_i \quad y_i]^\top + \alpha_p[x_f - x_i \quad y_f - y_i]^\top\right)$, with $\alpha = \frac{3}{t_f^2}t^2 - \frac{2}{t_f^3}t^3$, where x_i and x_f are the desired initial and final position of the path.
Super-Ellipse	$\mathbf{x} = v_p\begin{bmatrix} \lvert\cos(2\pi\omega_p t)\rvert^{2/m} a_p \text{sign}(\cos(2\pi\omega_p t)) \\ \lvert\sin(2\pi\omega_p t)\rvert^{2/n} b_p \text{sign}(\sin(2\pi\omega_p t)) \end{bmatrix}$, with $m = 5$, $n = 2$, $a_p = 3$, $b_p = 1$, and $\omega_p = \frac{4\pi}{t_f}$
Land Path	$\mathbf{x} = v_p\left([x_i \quad y_i \quad z_i]^\top + \alpha_p[x_f - x_i \quad y_f - y_i \quad z_f - z_i]^\top\right)$, with $\alpha = \frac{3}{t_f^2}t^2 - \frac{2}{t_f^3}t^3$.

To elucidate and validate the proposed approach, three robots are utilized: two ground robots and one aerial robot. Each robot in the formation performs an individual task, defined as a specific route. At a certain point, the robots initiate cooperative operations. The selected paths represent high-level sub-tasks performed by either a UGV or a UAV–UGV heterogeneous formation. The UAV is required to find the load, and the UGV B is required for the pickup/delivery task.

In the load transportation mission, each robot has a specific mission and a set of tasks that are represented in the state machine diagrams in Figure 12. The blocks that contain movement actions make use of the previously defined paths, as shown in Table 2. In general, the main UGV, known as "UGV A", starts its main mission by traveling along the initial delivery route for the packages to be transported. Along the way, it maps and identifies the objects in the work environment (see Figure 12a). When it identifies obstacles that prevent the task from continuing, it triggers a support call so that a UGV–UAV formation can assist in the process and the delivery mission can be successfully completed. In addition, UGV A is commanded to travel along a "meeting route", which in this work has been defined as a straight line (see Table 2) due to the characteristics of the obstacle considered in the proof of concept, as will be discussed in Section 4. At this point, the missions of the support UGV, known as "UGV B", and the UAV start up, are as described in Figure 12b,c.At first, UGV A must navigate along a predefined route until it reaches the "meeting route" defined for this robot, which is not the same as the route defined for UGV B, since there is an obstacle between them and the environment they are in, possibly with different characteristics and shapes, requiring dedicated path planning. The illustrative route defined for UGV B was defined as a super-ellipse (see Table 2). As the UGVs approach each other at a set distance, the UAV takes off and begins the process of collecting the cargo from UGV A and delivering it to UGV B. Throughout the process, information is exchanged between the agents and the GCS in order to determine the current progress of the mission and keep decision-making coherent. Once the packets have been transferred to UGV B, the UAV begins the process of landing on the mobile platform attached to the UGV, from which the UAV took off at the start of the mission. The algorithm dedicated to landing identifies and locates the platform and then adopts a trajectory tracking strategy (called "land path"; see Table 2) to reduce the distance between the UAV and the platform until it is safe to land. At the end, both UGVs are informed that the UAV has landed safely and that the packages have been transferred to UGV B as planned. Thus, UGV A returns to its command base, since it has finished its contribution to the main mission, which is the transportation of packages. On the other hand, the UGV–UAV formation still has to deliver the packages to the appropriate destination, and this becomes its task. At the end, the group returns to its respective command base, having completed the mission.

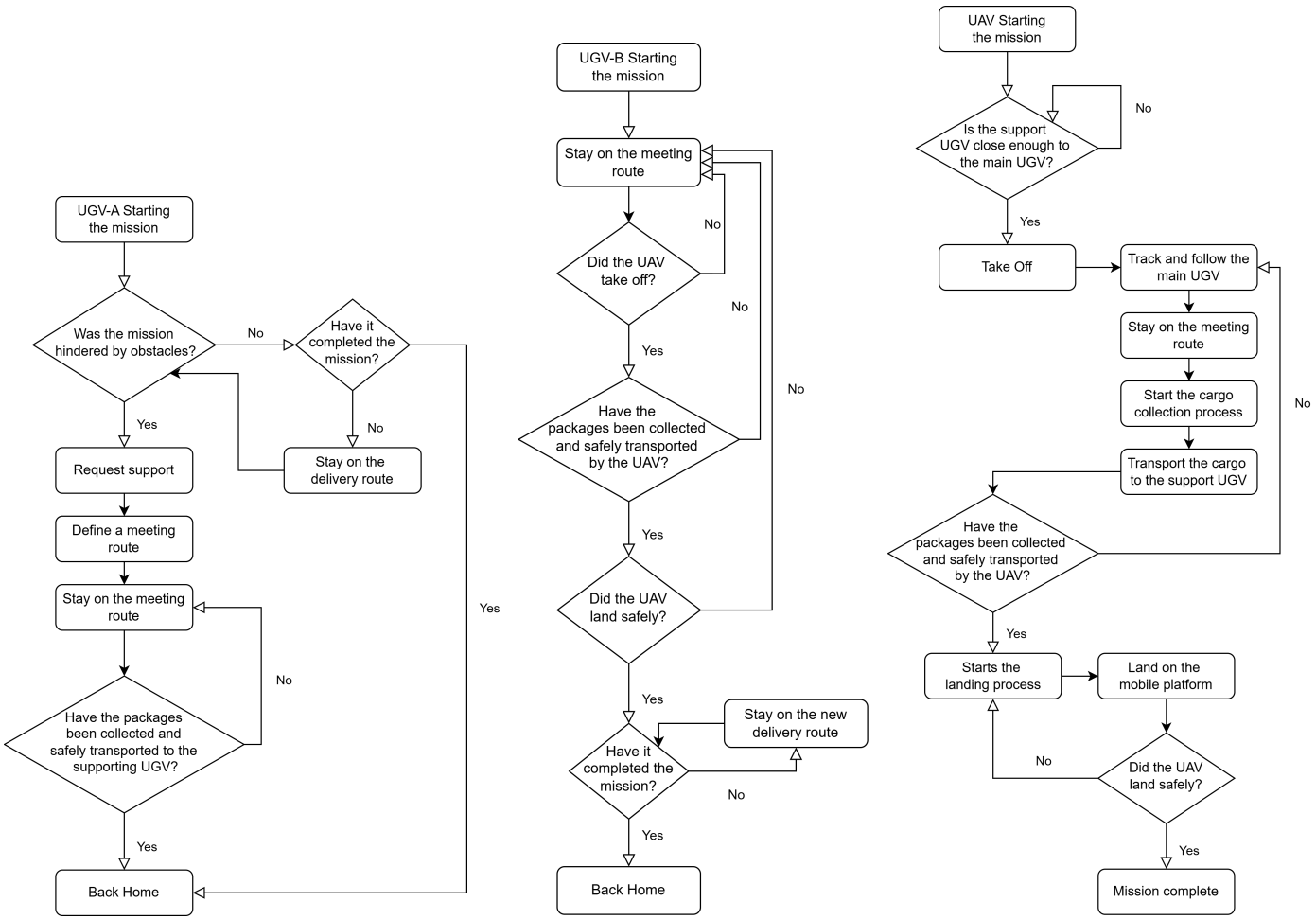

(**a**) UGB-A or main UGV. (**b**) UGV-B or support UGV. (**c**) UAV.

Figure 12. Task planning for each robot based on state machine representation.

4. Results and Discussion

Two experiments illustrate the functioning UAV–UGV cooperation for load transportation and the robot control performed using the system proposed here. In all the experiments, the UGVs move independently from other robots. Only the UAV has to worry about the exact position of both ground robots to perform the pickup and delivery of the loads. Such a setup clarifies the idea of an obstacle that UGVs are not able to overcome, and then the need for cooperation arises for a multi-robot system. The operation of the proposed strategy and the load transportation algorithm can be seen in the video of the full experiment, available at https://youtu.be/GDdqWQX0Hd8 (accessed on 7 January 2025). It is important to mention that the experimental load of 165 g, which corresponds to up to 36% of the UAV's mass, was chosen to validate the proof of concept using the available hardware, which includes a Bebop 2 drone with a limited payload capacity. While this weight is below the maximum capacity of commercial UAVs, the objective was to demonstrate the feasibility of collaborative transportation between robots using the well-known motion control laws, presented in this paper. For practical applications, the proposed system can be scaled to utilize UAVs and UGVs with greater payload capacities. Future work will involve experiments with heavier loads and upgraded robotic platforms to demonstrate applicability in real-world scenarios.

For each experiment, the sequence of actions can be checked, following the proposed strategy (Section 2.3). Table 3 provides a summary of the robots' actions for each step of the proposed strategy, the strategy commands, the aiming in the task, and time stamp.

Table 3. Sequence of events of the experiments. "Seq" indicates the sequence of the events, and "Time" indicates the moment (in mm:ss format) the action starts in the experiment.

Seq.	Time		Step	Action
	Exp 01	Exp 02		
	03:00	05:05	Start	Beginning of the experiment
1	03:04	05:10	Setup	The UGV A starts its mission, transporting the load
2	03:05	05:12	Assistance	UGV A meets the obstacle and requests support from UGV B, which initiates its movement towards the point closest to the obstacle
3	03:25	05:26	Collect Cargo	The UAV takes off and changes the reference point of the UAV and sends it to an estimated position above the UGV
4	03:39	05:45	Delivery	Collect the load and transport it to the top of the UGV B
5	04:04	06:20	Successful	While the UGVs are moving, the UAV lands on the trailer coupled to the UGV B
6	04:04	06:19	Go Home	UGV A goes to the GCS to finish its mission while UGV B transport the load
7	04:12	06:29	Transportation End	UGV B finishes its mission

These experiments show that with the implemented strategy, one can successfully coordinate a heterogeneous squadron to collect, transport, and deliver the load cooperatively, with the possibility that the UAV takes off and lands on the moving UGV.

The quadrotor's motion, crucial for the successful mission execution, is depicted in Figure 13a. While condensed within a tight time scale, the figure illustrates the entire trajectory executed by the UAV. The take-off action necessitates the fulfillment of specific stability constraints before it can commence execution. This explains the notable delay between the take-off set point value and the actual execution, a delay that is not evident during the subsequent smooth trajectory actions. Analyzing Figure 13, one can observe each stage in which the UAV is required to perform its task. When it is identified that the UGV B is close enough to the UGV A, the UAV takes off and initiates its mission tracking the UGV A. Once it has been able to estimate the position and velocity of UGV A, the UAV begins the process of collecting the load. Then, it delivers it to UGV B, and only then lands on the formation's trailer system, finishing the task. After completing their mission, both UGVs return to their GCSs.

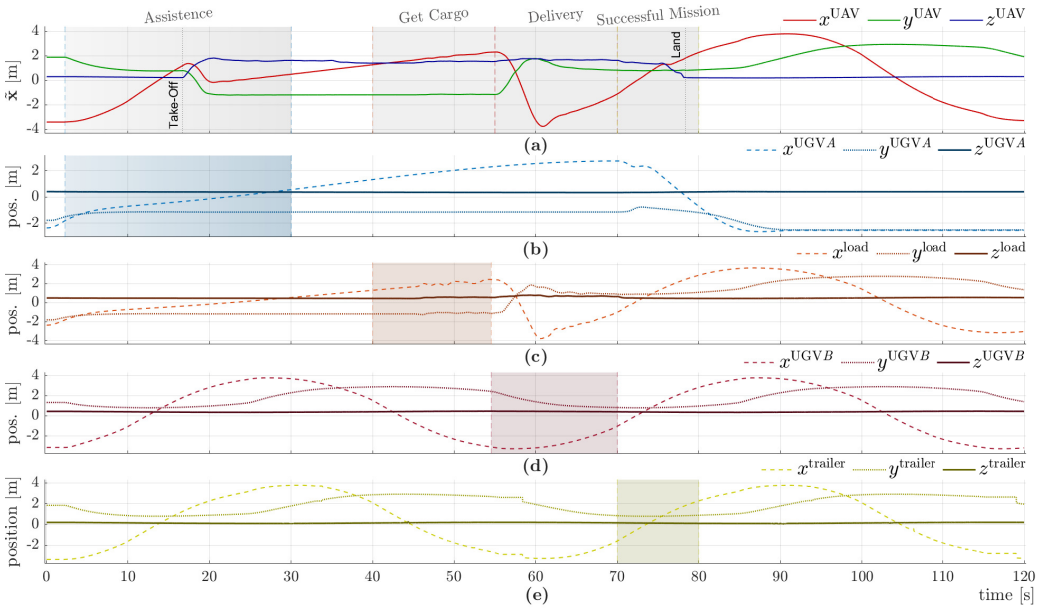

Figure 13. Tracking performance of the UAV: (**a**) **UAV** position; (**b**) **UGV A**; (**c**) load, (**d**) **UGV B**, and (**e**) trailer.

4.1. Robots' Behavior During Navigation

To make the proposed collaborative strategy clearer, this section discusses the behavior of each robot separately during the experiments. First of all, the **UGV A** robot is the one that performs the initial transportation of the load. During the execution of its mission, when reaching position $\mathbf{x}_o$, shown in Figure 14, it faces an insurmountable obstacle. From there, it starts a secondary mission, which aims to follow a path close to this obstacle while maintaining a safe distance. Given the prismatic profile of the obstacle, the planned path is a straight line (described in Table 2), starting at the point $\mathbf{x}_i$ and ending at $\mathbf{x}_f$. For validation purposes, it is assumed that by the last point of the reference, the load has already left **UGV A** and has been transported to **UGV B** by the **UAV**. With the lifting confirmation, **UGV A** returns to its command base (GCS), where it will wait for the assignment of a new mission.

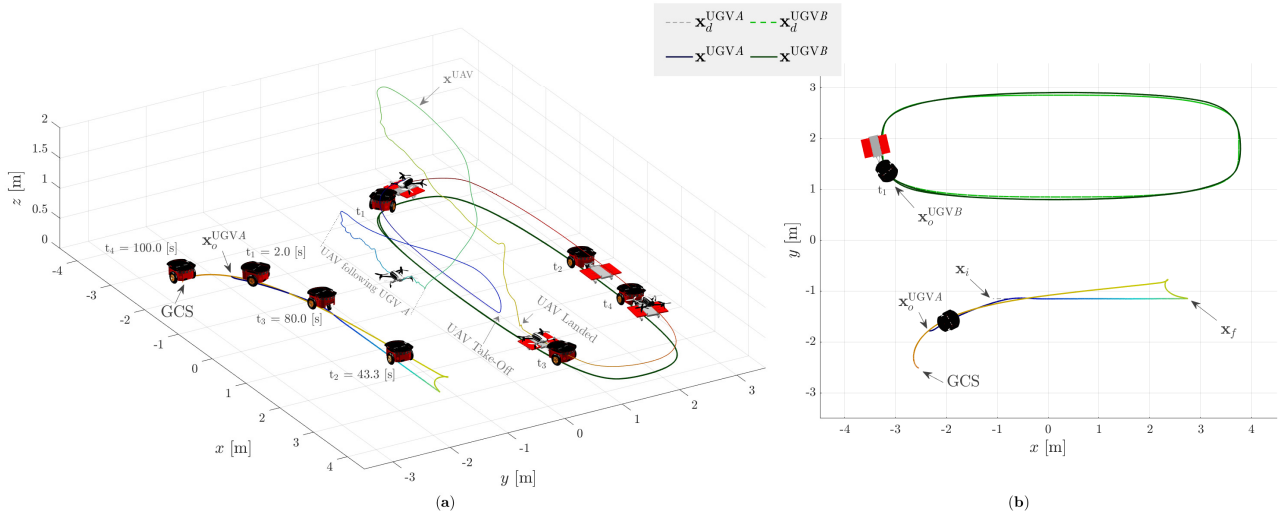

Figure 14. Tracking performance of the UGVs in the experiments. The gray dashed regions represent the period in which the robots are executing a stage of the strategy. Tracked positions for both UGVs: (**a**) real-time autonomous take-off, tracking, and landing of UAV on a moving UGV platform and (**b**) x-y view of the UGVs' performed routes and desired trajectory/positions.

Temporally, as illustrated in Figure 14a, at t_1, **UGV A** moves until it approaches the obstacle and then maintains a motion that enables the collection and transposition of the load; at t_2, the load is collected by the **UAV** and **UGV A** remains in its rectilinear motion until the **UAV** departs toward **UGV B**; at t_3, **UGV B** is returning to its GCS, after finishing its mission; and, finally, at t_4, **UGV A** has already reached its command base and is awaiting the delegation of a new task. Now, turning to **UGV B**, at the moment **UGV A** identifies the obstacle and approaches it, a command is sent to another GCS (in practical terms, the closest one after the obstacle) requesting a cooperation for transposing and delivering the package to the destination. At t_1, **UGV B** is allocated to supply the demand of **UGV A**. Thus, when approaching the obstacle, as stated earlier, **UGV A** maintains a smooth displacement, to make the load delivery while moving. When it becomes close enough to the obstacle, UAV takes off and meets **UGV A**. During the process of collecting the load, **UGV B** remains in motion, in this case, with a super-ellipse profile, as shown in Figure 14, at time instant t_2. After collecting the load, **UAV** navigates toward **UGV B** and makes the delivery to the designated location. Next, at time t_3, when the load has already been deposited on top of the **UGV B**, the UAV begins the process of landing on the trailer. For the rest of the experiment, **UGV B** carries the cargo on itself and **UAV**, as seen at time t_4. Finally, **UGV B** makes its way to the delivery destination and then returns to its respective GCS.

The main idea (contribution) of this paper is to demonstrate the execution of the collection and delivery of a load on ground robots, by lifting using a drone, with all agents

in motion. Although simplistic in terms of logistics, the experimental demonstration presented here is a proof of concept for a more advanced system with numerous branches of the carrier network and collection and delivery points, whose resource allocation strategy can adopt one of the strategies presented in [9,22,28]. In a broader context, a more complex system may be responsible for managing the transportation of load and optimizing the distribution of tasks according to the routes, agility, and load capacity of each vehicle.

The sensing and actuation capabilities of the robotic formation were designed for a controlled experimental setup. However, we recognize the need for robust sensing and actuation systems in real-world applications. For instance, advanced vision systems and LiDAR sensors could improve obstacle detection, object localization, and situational awareness. Actuation mechanisms with higher precision and reliability could enhance load manipulation and stability. Future work will explore these advancements, along with sensor fusion techniques and real-time decision-making algorithms, to address the challenges posed by complex and unpredictable environments.

4.2. Practical Issues Related to Perception and Navigation

Integrating the proposed application into urban environments characterized by terrain irregularities, moving obstacles, and interference from other vehicles, animals, and pedestrians necessitates the incorporation of advanced sensing technologies and sophisticated decision-making frameworks. Ground and aerial robots would benefit from high-resolution 3D mapping systems and obstacle detection technologies, such as LiDAR and stereo or monocular vision, to accurately perceive and navigate uneven terrain while identifying static and dynamic hazards [45,46]. The main challenges associated with these applications include the following: (*i*) achieving efficient and precise navigation within space-restricted, tight, and complex environments; (*ii*) developing path planning algorithms for multi-robot systems under diverse load conditions; (*iii*) reducing the high energy demand of robotic transportation systems; (*iv*) ensuring reliable online re-planning capabilities in dynamic and unpredictable scenarios; and (*v*) stabilizing large cable swings and load oscillations [47]. All of these challenges require extensive sensing and actuation capabilities, along with significant computational loads for perception and decision-making processes.

Understanding and mapping the terrain in the upcoming path of an aerial or a ground robot is one of the most challenging problems in field robotics. Vision-based techniques, including semantic segmentation and object detection algorithms, can help classify and prioritize obstacles, enabling the robot to make informed decisions [45]. To handle moving obstacles, such as pedestrians, cyclists, and vehicles, predictive motion-planning strategies like Dynamic Window Approach (DWA) [48,49], artificial potential fields [50–52], or trajectory prediction models based on recurrent neural networks (RNNs) [53,54] could be employed. These strategies allow robots to anticipate obstacle trajectories and adjust their path dynamically. Additionally, combining LiDAR data with computer vision can enhance environmental perception by fusing depth and semantic information, improving the reliability of navigation decisions in cluttered scenarios [55,56]. UAVs can complement ground robots by providing aerial assistance for obstacle detection, route optimization, and real-time monitoring [57–59]. Moreover, the integration of vehicle-to-vehicle (V2V) and vehicle-to-infrastructure (V2I) communication protocols would ensure seamless coordination among robots and infrastructure, improving safety and efficiency. These methodologies, although outside the scope of this work, represent essential advancements for applying the proposed approach to dynamic, complex urban environments.

5. Concluding Remarks

In summary, this work addresses the problem of cooperative load transportation by proposing a practical solution for autonomous navigation. We predefined high-level missions for a team composed of one UAV and two UGVs, simulating a typical last-mile delivery mission. The envisioned application scenario includes autonomous packet transportation, where the UAV is employed for picking and placing packets, while UGVs handle ground-based transportation. Our centralized robot coordination approach takes advantage of hierarchical task decomposition, addressing both low-level motion planning and high-level mission specifications within a multi-layered system.

These applications encompass urban, suburban, and rural delivery scenarios, where the cooperative control of UAVs and UGVs significantly enhances operational efficiency and reliability. Furthermore, the system's inherent versatility extends its suitability to diverse domains, including military, agricultural, industrial, and educational environments, underscoring its potential for intuitive and effective load transportation across a wide range of contexts.

As future work, we propose conducting a sensitivity analysis that could explore factors such as the maximum load the UAV can carry or the maximum speed the UGVs can navigate. This analysis would be valuable in identifying critical operational limits and optimizing the feasibility of UAV–UGV cooperative missions.

Author Contributions: Conceptualization, L.A.F.-J. and C.O.B.; methodology, L.A.F.-J.; validation, L.A.F.-J., C.O.B., and A.S.B.; data curation, L.A.F.-J. and C.O.B.; writing original draft preparation, L.A.F.-J.; writing, L.A.F.-J. and A.S.B., review and editing, A.S.B.; supervision, A.S.B.; project administration, A.S.B. and A.P.S.; funding acquisition, A.S.B. and A.P.S. All authors have read and agreed to the published version of the manuscript.

Funding: This work was financially supported by FAPEMIG-Fundação de Amparo à Pesquisa do Estado de Minas Gerais (Grant Number APQ-02573-21 and APQ-02282-24).

Institutional Review Board Statement: Not applicable.

Data Availability Statement: The data are available on request to interested readers.

Acknowledgments: The authors would like to thank the Conselho Nacional de Desenvolvimento Científico e Tecnológico (CNPq), an agency of the Brazilian Ministry of Science, Technology, Innovations and Communications that supports scientific and technological development, as well as the Fundação de Amparo à Pesquisa e Inovação de Minas Gerais (FAPEMIG), an agency of the State of MG, Brazil, that supports scientific and technological development, for financing this project. Fagundes would like to thank the FAPEMIG for the scholarship that allowed him to develop his studies. Barcelos and Fagundes-Junior thank CAPES- Coordenação de Aperfeiçoamento de Pessoal de Nível Superior- and FAPEMIG- Fundação de Amparo à Pesquisa do Estado de Minas Gerais-, respectively, for their scholarships.

Conflicts of Interest: The authors declare no conflicts of interest.

References

1. Gupta, A.; Afrin, T.; Scully, E.; Yodo, N. Advances of UAVs toward future transportation: The State-of-the-Art, challenges, and Opportunities. *Future Transp.* **2021**, *1*, 326–350. [CrossRef]
2. Cortes, J.D.; Suzuki, Y. Last-mile delivery efficiency: En route transloading in the parcel delivery industry. *Int. J. Prod. Res.* **2022**, *60*, 2983–3000. [CrossRef]
3. Barakou, S.C.; Tzafestas, C.S.; Valavanis, K.P. A Review of Real-Time Implementable Cooperative Aerial Manipulation Systems. *Drones* **2024**, *8*, 196. [CrossRef]
4. Nguyen, V.S.; Jung, J.; Jung, S.; Joe, S.; Kim, B. Deployable hook retrieval system for UAV rescue and delivery. *IEEE Access* **2021**, *9*, 74632–74645. [CrossRef]

5. Estevez, J.; Garate, G.; Lopez-Guede, J.M.; Larrea, M. Review of aerial transportation of suspended-cable payloads with quadrotors. *Drones* **2024**, *8*, 35. [CrossRef]
6. Ollero, A.; Tognon, M.; Suarez, A.; Lee, D.; Franchi, A. Past, present, and future of aerial robotic manipulators. *IEEE Trans. Robot.* **2021**, *38*, 626–645. [CrossRef]
7. Villa, D.K.; Brandão, A.S.; Sarcinelli-Filho, M. Load transportation using quadrotors: A survey of experimental results. In Proceedings of the 2018 International conference on unmanned aircraft systems (ICUAS), Dallas, TX, USA, 12–15 June 2018; pp. 84–93.
8. Pizetta, I.H.B.; Brandão, A.S.; Sarcinelli-Filho, M. Cooperative load transportation using three quadrotors. In Proceedings of the 2019 International Conference on Unmanned Aircraft Systems (ICUAS), Atlanta, GA, USA, 11–14 June 2019; pp. 644–650.
9. Jin, X.; Hu, Z. Adaptive Cooperative Load Transportation by a Team of Quadrotors With Multiple Constraint Requirements. *IEEE Trans. Intell. Transp. Syst.* **2022**, *24*, 801–814. [CrossRef]
10. Michael, N.; Fink, J.; Kumar, V. Cooperative manipulation and transportation with aerial robots. *Auton. Robot.* **2011**, *30*, 73–86. [CrossRef]
11. Sreenath, K.; Kumar, V. Dynamics, control and planning for cooperative manipulation of payloads suspended by cables from multiple quadrotor robots. *Robot. Sci. Syst.* **2013**.
12. Tang, S.; Sreenath, K.; Kumar, V. Multi-robot trajectory generation for an aerial payload transport system. In *Robotics Research*; Springer: Berlin/Heidelberg, Germany, 2020; pp. 1055–1071.
13. Ritz, R.; D'Andrea, R. Carrying a flexible payload with multiple flying vehicles. In Proceedings of the 2013 IEEE/RSJ International Conference on Intelligent Robots and Systems, Tokyo, Japan, 3–7 November 2013; pp. 3465–3471.
14. Augugliaro, F.; Lupashin, S.; Hamer, M.; Male, C.; Hehn, M.; Mueller, M.W.; Willmann, J.S.; Gramazio, F.; Kohler, M.; D'Andrea, R. The flight assembled architecture installation: Cooperative construction with flying machines. *IEEE Control Syst. Mag.* **2014**, *34*, 46–64.
15. Munasinghe, I.; Perera, A.; Deo, R.C. A Comprehensive Review of UAV-UGV Collaboration: Advancements and Challenges. *J. Sens. Actuator Netw.* **2024**, *13*, 81. [CrossRef]
16. Vu, Q.; Raković, M.; Delic, V.; Ronzhin, A. Trends in development of UAV-UGV cooperation approaches in precision agriculture. In Proceedings of the Interactive Collaborative Robotics: Third International Conference, ICR 2018, Leipzig, Germany, 18–22 September 2018; Proceedings 3; Springer: Berlin/Heidelberg, Germany, 2018; pp. 213–221.
17. Chen, Z.; Hou, S.; Wang, Z.; Chen, Y.; Hu, M.; Ikram, R.M.A. Delivery Route Scheduling of Heterogeneous Robotic System with Customers Satisfaction by Using Multi-Objective Artificial Bee Colony Algorithm. *Drones* **2024**, *8*, 519. [CrossRef]
18. Liu, C.; Zhao, J.; Sun, N. A review of collaborative air-ground robots research. *J. Intell. Robot. Syst.* **2022**, *106*, 60. [CrossRef]
19. Chai, R.; Guo, Y.; Zuo, Z.; Chen, K.; Shin, H.S.; Tsourdos, A. Cooperative motion planning and control for aerial-ground autonomous systems: Methods and applications. *Prog. Aerosp. Sci.* **2024**, *146*, 101005. [CrossRef]
20. Chiang, W.C.; Li, Y.; Shang, J.; Urban, T.L. Impact of drone delivery on sustainability and cost: Realizing the UAV potential through vehicle routing optimization. *Appl. Energy* **2019**, *242*, 1164–1175. [CrossRef]
21. Schneider, D. The delivery drones are coming. *IEEE Spectr.* **2020**, *57*, 28–29. [CrossRef]
22. Huang, H.; Hu, C.; Zhu, J.; Wu, M.; Malekian, R. Stochastic Task Scheduling in UAV-Based Intelligent On-Demand Meal Delivery System. *IEEE Trans. Intell. Transp. Syst.* **2021**, *23*, 13040–13054. [CrossRef]
23. She, R.; Ouyang, Y. Efficiency of UAV-based last-mile delivery under congestion in low-altitude air. *Transp. Res. Part C Emerg. Technol.* **2021**, *122*, 102878. [CrossRef]
24. Ghamry, K.A.; Dong, Y.; Kamel, M.A.; Zhang, Y. Real-time autonomous take-off, tracking and landing of UAV on a moving UGV platform. In Proceedings of the 24th Mediterranean Conference on Control and Automation, MED, Athens, Greece, 21–24 June 2016; pp. 1236–1241. [CrossRef]
25. Bai, X.; Cao, M.; Yan, W.; Ge, S.S. Efficient Routing for Precedence-Constrained Package Delivery for Heterogeneous Vehicles. *IEEE Trans. Autom. Sci. Eng.* **2020**, *17*, 248–260. [CrossRef]
26. Das, D.N.; Sewani, R.; Wang, J.; Tiwari, M.K. Synchronized truck and drone routing in package delivery logistics. *IEEE Trans. Intell. Transp. Syst.* **2020**, *22*, 5772–5782. [CrossRef]
27. Bacheti, V.P.; Brandao, A.S.; Sarcinelli-Filho, M. A Path-Following Controller for a UAV-UGV Formation Performing the Final Step of Last-Mile-Delivery. *IEEE Access* **2021**, *9*, 142218–142231. [CrossRef]
28. Sawadsitang, S.; Niyato, D.; Tan, P.S.; Wang, P. Joint ground and aerial package delivery services: A stochastic optimization approach. *IEEE Trans. Intell. Transp. Syst.* **2018**, *20*, 2241–2254. [CrossRef]
29. Arbanas, B.; Ivanovic, A.; Car, M.; Haus, T.; Orsag, M.; Petrovic, T.; Bogdan, S. Aerial-ground robotic system for autonomous delivery tasks. In Proceedings of the 2016 IEEE international conference on robotics and automation (ICRA), Stockholm, Sweden, 16–21 May 2016; pp. 5463–5468.
30. Arbanas, B.; Ivanovic, A.; Car, M.; Orsag, M.; Petrovic, T.; Bogdan, S. Decentralized planning and control for UAV–UGV cooperative teams. *Auton. Robot.* **2018**, *42*, 1601–1618. [CrossRef]

31. Guérin, F.; Guinand, F.; Brethé, J.F.; Pelvillain, H. UAV-UGV cooperation for objects transportation in an industrial area. In Proceedings of the 2015 IEEE International Conference on Industrial Technology (ICIT), Seville, Spain, 17–19 March 2015; pp. 547–552.
32. Brandão, A.S.; Sarcinelli-Filho, M.; Carelli, R. Leader-following control of a UAV-UGV formation. In Proceedings of the 2013 16th International Conference on Advanced Robotics (ICAR), Montevideo, Uruguay, 25–29 November 2013; pp. 1–6.
33. De La Cruz, C.; Carelli, R. Dynamic model based formation control and obstacle avoidance of multi-robot systems. *Robotica* **2008**, *26*, 345–356. [CrossRef]
34. Martins, F.N.; Sarcinelli-Filho, M.; Carelli, R. A velocity-based dynamic model and its properties for differential drive mobile robots. *J. Intell. Robot. Syst.* **2017**, *85*, 277–292. [CrossRef]
35. de Carvalho, K.B.; Villa, D.K.D.; Sarcinelli-Filho, M.; Brandão, A.S. Gestures-teleoperation of a heterogeneous multi-robot system. *Int. J. Adv. Manuf. Technol.* **2022**, *118*, 1999–2015. [CrossRef]
36. Tang, S.; Kumar, V. Autonomous flight. *Annu. Rev. Control. Robot. Auton. Syst.* **2018**, *1*, 29–52. [CrossRef]
37. Pinto, A.O.; Marciano, H.N.; Bacheti, V.P.; Moreira, M.S.M.; Brandão, A.S.; Sarcinelli-Filho, M. High-Level Modeling and Control of the *Bebop 2* Micro Aerial Vehicle. In Proceedings of the The 2020 International Conference on Unmanned Aircraft Systems, Athens, Greece, 1–4 September 2020; pp. 939–947. [CrossRef]
38. Lieret, M.; Kogan, V.; Döll, S.; Franke, J. Automated in-house transportation of small load carriers with autonomous unmanned aerial vehicles. In Proceedings of the 2019 IEEE 15th International Conference on Automation Science and Engineering (CASE), Vancouver, BC, Canada, 22–26 August 2019; pp. 1010–1015.
39. Orgeira-Crespo, P.; Rey, G.; Pousada, P.R.; Aguado-Agelet, F. Transport of Light Parts for Logistics Supply in Industrial Manufacturing Plants by Means of UAV. In *Applying Drones to Current Societal and Industrial Challenges*; Springer: Berlin/Heidelberg, Germany, 2024; pp. 155–180.
40. Miranda, V.R.; Rezende, A.M.; Rocha, T.L.; Azpúrua, H.; Pimenta, L.C.; Freitas, G.M. Autonomous navigation system for a delivery drone. *J. Control. Autom. Electr. Syst.* **2022**, *33*, 141–155. [CrossRef]
41. Stein, A.; Vexler, D.; Singh, T. ArUco Based Reference Shaping for Real-time Precision Motion Control for Suspended Payloads. In Proceedings of the 2024 American Control Conference (ACC), Toronto, ON, Canada, 10–12 July 2024; pp. 4390–4395.
42. Lebedev, I.; Erashov, A.; Shabanova, A. Accurate autonomous uav landing using vision-based detection of aruco-marker. In Proceedings of the International Conference on Interactive Collaborative Robotics, Athens, Greece, 21–24 June 2020; Springer: Berlin/Heidelberg, Germany, 2020; pp. 179–188.
43. Khazetdinov, A.; Zakiev, A.; Tsoy, T.; Svinin, M.; Magid, E. Embedded ArUco: A novel approach for high precision UAV landing. In Proceedings of the 2021 International Siberian Conference on Control and Communications (SIBCON), Kazan, Russia, 13–15 May 2021; pp. 1–6.
44. Wang, J.; McKiver, D.; Pandit, S.; Abdelzaher, A.F.; Washington, J.; Chen, W. Precision uav landing control based on visual detection. In Proceedings of the 2020 IEEE Conference on Multimedia Information Processing and Retrieval (MIPR), Shenzhen, China, 6–8 August 2020; pp. 205–208.
45. Borges, P.V.; Peynot, T.; Liang, S.; Arain, B.; Wildie, M.; Minareci, M.; Lichman, S.; Samvedi, G.; Sa, I.; Hudson, N.; et al. A Survey on Terrain Traversability Analysis for Autonomous Ground Vehicles: Methods, Sensors, and Challenges. *Field Robot.* **2022**, *2*, 1567–1627. [CrossRef]
46. Trevelyan, J.; Hamel, W.R.; Kang, S.C. Robotics in Hazardous Applications. In *Springer Handbook of Robotics*; Springer International Publishing: Cham, Switzerland, 2016; pp. 1521–1548. [CrossRef]
47. Leong, P.Y.; Ahmad, N.S. Exploring Autonomous Load-Carrying Mobile Robots in Indoor Settings: A Comprehensive Review. *IEEE Access* **2024**, *12*, 131395–131417. [CrossRef]
48. Chang, L.; Shan, L.; Jiang, C.; Dai, Y. Reinforcement based mobile robot path planning with improved dynamic window approach in unknown environment. *Auton. Robot.* **2021**, *45*, 51–76. [CrossRef]
49. Kim, J.; Yang, G.H. Improvement of dynamic window approach using reinforcement learning in dynamic environments. *Int. J. Control. Autom. Syst.* **2022**, *20*, 2983–2992. [CrossRef]
50. Nekoo, S.; Acosta, J.; Ollero, A. Collision avoidance of SDRE controller using artificial potential field method: Application to aerial robotics. In Proceedings of the 2020 International Conference on Unmanned Aircraft Systems (ICUAS), Athens, Greece, 1–4 September 2020; pp. 551–556.
51. Sudhakara, P.; Ganapathy, V.; Priyadharshini, B.; Sundaran, K. Obstacle avoidance and navigation planning of a wheeled mobile robot using amended artificial potential field method. *Procedia Comput. Sci.* **2018**, *133*, 998–1004. [CrossRef]
52. Pashna, M.; Yusof, R.; Ismail, Z.H.; Namerikawa, T.; Yazdani, S. Autonomous multi-robot tracking system for oil spills on sea surface based on hybrid fuzzy distribution and potential field approach. *Ocean Eng.* **2020**, *207*, 107238. [CrossRef]
53. Capobianco, S.; Millefiori, L.M.; Forti, N.; Braca, P.; Willett, P. Deep learning methods for vessel trajectory prediction based on recurrent neural networks. *IEEE Trans. Aerosp. Electron. Syst.* **2021**, *57*, 4329–4346. [CrossRef]

54. Messaoud, K.; Yahiaoui, I.; Verroust-Blondet, A.; Nashashibi, F. Relational recurrent neural networks for vehicle trajectory prediction. In Proceedings of the 2019 IEEE Intelligent Transportation Systems Conference (ITSC), Auckland, New Zealand, 27–30 October 2019; pp. 1813–1818.
55. Debeunne, C.; Vivet, D. A review of visual-LiDAR fusion based simultaneous localization and mapping. *Sensors* **2020**, *20*, 2068. [CrossRef] [PubMed]
56. Xu, X.; Zhang, L.; Yang, J.; Cao, C.; Wang, W.; Ran, Y.; Tan, Z.; Luo, M. A review of multi-sensor fusion slam systems based on 3D LIDAR. *Remote Sens.* **2022**, *14*, 2835. [CrossRef]
57. Kim, J.H.; Kwon, J.W.; Seo, J. Multi-UAV-based stereo vision system without GPS for ground obstacle mapping to assist path planning of UGV. *Electron. Lett.* **2014**, *50*, 1431–1432. [CrossRef]
58. Hernandez, A.; Copot, C.; Cerquera, J.; Murcia, H.; De Keyser, R. Formation control of UGVs using an UAV as remote vision sensor. *IFAC Proc. Vol.* **2014**, *47*, 11872–11877. [CrossRef]
59. Li, P.; Li, W.; Cui, Z.; Yang, P.; Chen, C.; You, B.; Wang, J. UGV Navigation in Complex Environment: An Approach Integrating Security Detection and Obstacle Avoidance Control. *IEEE Trans. Intell. Veh.* **2024**, 1–14. [CrossRef]